HHS Public Access

Author manuscript

Arterioscler Thromb Vasc Biol. Author manuscript; available in PMC 2019 April 01.

Published in final edited form as:

Arterioscler Thromb Vasc Biol. 2018 April ; 38(4): 843–853. doi:10.1161/ATVBAHA.117.309897.

A novel role of IL-1β in NETosis and Abdominal Aortic Aneurysms

Akshaya K. Meher[1,2,3], **Michael Spinosa**[1], **John P. Davis**[1], **Nicolas Pope**[1], **Victor E. Laubach**[1], **Gang Su**[1], **Vlad Serbulea**[2], **Norbert Leitinger**[2,3], **Gorav Ailawadi**[1,3,5], and **Gilbert R. Upchurch Jr.**[1,3,4]

[1]Department of Surgery, University of Virginia, Charlottesville, Virginia, USA

[2]Department of Pharmacology, University of Virginia, Charlottesville, Virginia, USA

[3]Robert M. Berne Cardiovascular Research Center, University of Virginia, Charlottesville, Virginia, USA

[4]Department of Molecular Physiology and Biological Physics, University of Virginia, Charlottesville, Virginia, USA

[5]Department of Biomedical Engineering, University of Virginia, Charlottesville, Virginia, USA

Abstract

Objective—Neutrophils promote experimental abdominal aortic aneurysm (AAA) formation *via* a mechanism that is independent from matrix metalloproteinases. Recently, we reported a dominant role of IL-1β in the formation of murine experimental AAAs. Here, the hypothesis that IL-1β-induced neutrophil extracellular trap formation (NETosis) promotes AAA was tested.

Approach and Results—NETs were identified through co-localized staining of neutrophil, citrullinated histone H3 (Cit-H3), and DNA, using immunohistochemistry. NETs were detected in human AAAs and were co-localized with IL-1β. *In vitro*, IL-1RA attenuated IL-1β-induced NETosis in human neutrophils. Mechanistically, IL-1β treatment of isolated neutrophils induced nuclear localization of ceramide synthase 6 and synthesis of C16-ceramide, which was inhibited by IL-1RA or Fumonicin B1, an inhibitor of ceramide synthesis. Furthermore, IL-1RA or Fumonicin B1 attenuated IL1-β-induced NETosis. In an experimental model of murine AAA, NETs were detected at a very early stage–day 3 of aneurysm induction. IL-1β knockout mice demonstrated significantly lower infiltration of neutrophils to aorta and were protected from AAA. Adoptive transfer of wild-type neutrophils promoted AAA formation in IL-1β knockout mice. Moreover, treatment of wild-type mice with Cl-amidine, an inhibitor NETosis, significantly attenuated AAA formation, whereas, treatment with deoxyribonuclease, a DNA digesting enzyme, had no effect on AAA formation.

Conclusion—Altogether, the results suggest a dominant role of IL-1β-induced NETosis in AAA formation.

Address correspondence to: Akshaya K. Meher, Ph.D., Department of Pharmacology, University of Virginia, P.O. Box 800735, Charlottesville, VA 22908, Phone: (434) 243-6386, Fax: (434) 982-3878, am5bv@virginia.edu.

DISCLOSURES

None

Keywords

Abdominal aortic aneurysm; Neutrophil; NETosis; IL-1β and ceramide

Subject codes

Cardiovascular Surgery and Aneurysm

INTRODUCTION

Abdominal aortic aneurysm (AAA) is common in men aged 65 and older. Major risk factors for AAA formation include smoking, hypertension, atherosclerosis and hypercholesterolemia[1]. So far, no nonsurgical therapy is available to slow the growth of AAA or prevent rupture. Surgical repair (open or endovascular) is associated with a high risk of death and systemic inflammation. Therefore, it is pertinent to understand the mechanisms of AAA growth and rupture in order to develop a treatment therapy.

The host immune system plays a leading role in AAA formation by recruiting immune cells to the aortic media and adventitia. During AAA formation, aortic medial and adventitial layers undergo major pathological changes with degradation of extracellular matrix and marked infiltration of inflammatory cells, such as neutrophils, T cells, B cells, macrophages, mast cells, natural killer cells and dendritic cells[2, 3]. Although initial stages of AAA growth in humans are undefined, in experimental models of murine AAAs, we have previously reported infiltration of a predominant number of neutrophils to aorta at the early stages of aneurysm formation[4]. Furthermore, treatment of wild-type (WT) mice with anti-polymorphonuclear (anti-PMN) antibody caused systemic neutropenia and protected mice from AAA induced by the elastase perfusion model[4]. Interestingly, no decrease in MMP2 or 9 level was found in the AAA of neutropenic mice compared to the WT mice. These results strongly suggest a critical role of neutrophils in AAA formation.

Apart from phagocytosis and degranulation, neutrophil extracellular trap formation (NETosis) is another part of the neutrophil-mediated defense mechanism. While NETosis is beneficial for entrapment and clearance of pathogens, induction of NETosis in sterile inflammation is deleterious for many chronic diseases including atherosclerosis[5], gout[6] and systemic inflammatory response syndrome[7]. Recently, Yan et al. claimed that the co-localized staining of myeloperoxidase, histone and DNA are representative of NETs in mouse AAA formed in day 2 after elastase perfusion[8]. However, macrophages can also infiltrate the aorta at the same time as neutrophils, can synthesize myeloperoxidase, and form extracellular traps[9, 10]. Therefore, it remains elusive whether NETs are present and contribute to AAA formation in human and experimental models of mouse AAAs. Furthermore, identification of a possible trigger of NETosis in AAA is critical for development of a treatment strategy.

Using murine experimental AAA models, we have recently shown that IL-1β and IL-1R are essential for formation AAA and attenuation of developing AAA, respectively[11]. We found that 3 days following elastase perfusion, aortic IL-1β protein level was significantly higher

than control mice, which coincides with the recruitment of neutrophils to AAA. Both genetic deficiency of IL-1β (IL-1β KO mouse) and pharmacological inhibition of IL-1β binding to IL-1 receptor (*via* IL-1RA/Anakinra treatment) protected mice from AAA formation, with decreased aortic infiltration of neutrophils and macrophages, indicating requirement of aortic IL-1β synthesis for AAA formation. IL-1β has been shown to induce NETosis *in vitro*[7]. These results together suggest that infiltrating neutrophils are potentially exposed to high concentration of IL-1β in AAA tissue and undergo NETosis.

Ceramides are known as messenger molecules. Some of the long-chain ceramides, such as C16-ceramide, can form channels on the mitochondrial membrane and induce apoptosis[12]. Ceramide synthase S6 (CerS6), the C16-ceramide synthesizing enzyme, is localized in the perinuclear region and is implicated in increasing permeability of the nuclear membrane[13]. Interestingly, IL-1β is known to induce ceramide synthesis[14], however, it is unknown if IL-1β induces ceramide synthesis in neutrophils.

Here, we examined whether IL-1β induces NETosis *via* increasing C16-ceramide synthesis and tested the hypothesis that IL-1β-induced NETosis promotes AAA formation. So far, NETosis is quantified in *in vitro* experiments by manual counting of normal nuclei and nuclei that form net-like structures[8]. This method is highly error prone because, because once NETs are formed, they lose their normal rounded and defined structure, and may cluster together, leading to a miscalculation of the number of nuclei that have undergone NETosis. Herein, we developed a new method of quantifying NETosis using the ImageJ program which can be widely used for NETosis studies performed *in vitro*.

MATERIALS AND METHODS

Human tissue collection, immunohistochemistry of aortic sections and ANCA quantification from plasma

Collection of human aortic tissue, blood and plasma was approved by University of Virginia Institutional Review Board for Health Sciences Research (IRB# 17042). Human abdominal aortic aneurysm (AAA) tissues were collected from patients undergoing open AAA repair and control aortic tissues were collected from healthy organ donors. A part of the aortic tissue was fixed in formalin and embedded in paraffin for immunohistochemistry and another part was frozen and stored in −80 °C for Western blotting. Blood was collected in EDTA-containing collection tubes and immediately centrifuged to collect plasma, which was stored in −80 °C.

For immunohistochemistry, 5 μM cross sections of the paraffin embedded aortic tissue were cut and standard methods of deparaffinization and antigen retrieval were performed. For immunoperoxidase staining, the aortic sections were treated with hydrogen peroxide soon after deparaffinization. Following antigen retrieval, the sections were blocked with a blocking buffer containing 10% donkey serum and Avidin/Biotin blocking kit (SP-2001, Vector Laboratories), and then treated with primary antibodies for overnight at 4 °C. Subsequently, the sections were washed, treated with biotin-conjugated secondary antibody, VECTASTAIN Elite ABC Kit (PK-6100, Vector Laboratories), and finally stained with DAB solution (SK-4105, Vector Laboratories). Nuclei were visualized using hematoxylin

and eosin staining. A permanent mounting medium with cover slip was applied before imaging.

For immunofluorescence studies, the aortic sections were blocked with 1% donkey serum, 1% bovine serum albumin and 0.3M Glycine in TBST (Tris buffer saline containing 0.1% Tween 20) buffer, treated with the primary antibodies in blocking buffer for overnight at 4 °C, washed in TBST, treated with fluorescent-conjugated secondary antibody for 2 hours at room temperature before mounting with 1 μM DNA dye Yo-Pro-1 (Yo-Pro-1 Iodide, Y3603, ThermoFisher Scientific) in VECTASHIELD Mounting Medium (H-1000, Vector Laboratories). The primary antibodies used were Anti-Neutrophil Elastase antibody (ab68672, Abcam), Anti-Histone H3 (citrulline R2 + R8 + R17) (ab5103, Abcam). The secondary antibodies were Alexa Fluor 555 Donkey Anti-Rabbit IgG (A-31572, Life Technologies) and Alexa Fluor 488 Donkey Anti-Mouse IgG (A-21202, Life Technologies). As a negative control, one out of the three AAA sections on a slide was excluded for the primary antibody and staining was performed. Images were acquired on an inverted Zeiss LSM 700 and images were analyzed using ZEN 2012 software.

Isolation of human neutrophils, flow cytometry, induction of NETosis and NET quantification

Blood from healthy humans was collected and experiments were performed following the guidelines for University of Virginia Institutional Review Board for Health Sciences Research. Neutrophils were isolated from human blood using a stand protocol. Briefly, freshly collected blood was layered in the top of Histopaque gradients Histopaque-1119 and -1077 (11191 and 10771, Sigma-Aldrich, St. Louis, MO), and centrifuged at 700g for 30 min at room temperature. After aspirating the top mononuclear layer, the middle polymorphonuclear (PMN) layer was collected without disturbing the bottom red blood cell layer. Contaminating RBCs were lysed in the PMN layer and the cells were suspended in complete RPMI medium containing 2 mM L-glutamine, 0.5% fetal bovine serum, 1% antibiotic-antimycotic and 20 mM HEPES. The cells were incubated at 37 °C and 5% CO_2 in a humidified incubator and used for NETosis studies after 30–60 min of isolation.

To determine the concentration of neutrophils in the PMN preparation, 1 million cells from whole blood (following lysis of red blood cells), monocyte layer and PMN layer were stained with FITC anti-human CD66b Antibody (50-166-209, Fisher Scientific, Waltham, MA), Alexa Fluor 647 anti-human CD16 Antibody (50-165-796, Fisher Scientific) and DAPI (D1306, Invitrogen, Carlsbad, CA), run on a Becton Dickinson LSRFortessa flow cytometer and analyzed using FlowJo 7.6.5.

To induce NETosis and examine the effect of inhibitors of IL-1β signaling and of ceramide synthesis pathway, 0.5 million cells are seeded on poly-lysine-treated cover glasses, and pre-treated with vehicle, IL-1RA (100 ng/ml, Kineret, SOBI, Waltham, MA), Myriocin (5 μM) or Fumonicin B1 (10 μM) (Cayman Chemicals, Ann Arbor, MI) for 30 min and then treated with various concentrations of IL-1β for 3 hours. Following the treatment, medium was carefully removed and the cells were fixed with 4% paraformaldehyde. The cells were permeabilized with TBST and stained with Anti-Neutrophil Elastase antibody or Anti-Histone H3 (citrulline R2 + R8 + R17) and Yo-Pro-1 as described earlier. For ceramide and

CerS6 staining, following IL-1β or IL-1RA treatment, the cells were fixed and permeabilized using ice cold acetone: methanol (1:1) for 10 min. The cells were stained with Monoclonal Anti-Ceramide antibody, clone MID 15B4 (C8104-50TST, Sigma-Aldrich) or LASS6 Antibody (Ceramide synthase S6 or CerS6), clone L-18 (sc-100554, Santa Cruz Biotechnology, Dallas, TX) and the secondary antibodies Alexa Fluor 488 Goat Anti-Mouse IgM (A-21042, Life Technologies, Carlsbad, CA) or Alexa Fluor 488 Donkey Anti-Mouse IgG (A-21202, Life Technologies). VECTASHIELD Mounting Medium containing DAPI (H-1200, Vector Laboratories) was used to mount the slides before imaging. As a negative control, primary antibodies were excluded and the cells were stained with secondary antibodies.

To quantify NETosis, after fixation and permeabilization, neutrophil-DNA was stained with DAPI, images were acquired on Zeiss LSM 700 using ZEN 2012 and analyzed using ImageJ software. In the analysis, first the total DNA+ area was determined via keeping particle size to 0-∞, and then total nuclear area was determined by decreasing the threshold and increasing the particle size to 100-∞. NETosis was calculated as the ratio of DNA+ area to the nuclear area. To validate our new NETosis quantification method, we quantified NET-DNA released by neutrophils after induction of NETosis, as described by others[15, 16]. Briefly, 6 hours after various treatments (as described in supplemental figure IV) on 200 μl of 1 million human neutrophils in complete RPMI medium seeded on a round bottom 96 well plate, the plate was centrifuged at 500g for 10 minutes at 4 °C, 100 μl of supernatant was collected and used immediately for quantification of double stranded DNA (dsDNA) using diluted Quant-iT™ PicoGreen™ dsDNA Reagent (Cat. No. P7581, ThermoFisher Scientific) as described by the manufacturer.

Isolation of ceramides from human aorta and neutrophils

Frozen aortic tissues collected from human AAA and healthy organ donors were homogenized in ice cold phosphate buffer saline. Next, 200 μL of chloroform was added to the homogenate, and the homogenate was incubated overnight at 48 °C. After cooling to room temperature, 20μL of 1M KOH in methanol was added, and the samples were incubated at 37 °C for 2h. Lipids were neutralized with 5 μL of glacial acetic acid. 1.5 mL of HPLC-grade chloroform and 2 mL of H_2O (Fisher Scientific, Waltham, MA) were added to each sample, vortexed, and centrifuged at 1500g for 10 min to separate the organic and aqueous phases. The organic phase was dried under argon prior to resuspension in mobile phase solvent containing 97% acetonitrile, 2% methanol, and 1% formic acid (v/v/v) supplemented with 5 mM ammonium formate.

To extract ceramides from isolated human neutrophils, following treatments, 3 million cells were washed and suspended in ice cold PBS. Ceramides were extracted as described for aortic tissue. In both of the procedures, 500 picomoles of C17 Ceramide (d18:1/17:0) (Avanti Polar Lipids, Alabaster, AL) was added as an internal standard.

LC-MS Measurement

Using a triple quadrupole mass spectrometer (Applied Biosystems 4000 Q-Trap) coupled to a Shimadzu LC-20AD LC system equipped with a Supelcosil LC NH2 column (50 cm×2.1

mm, 3μm) samples were subjected to normal phase LC-MS/MS. A multiple reaction monitoring scheme for naturally occurring species of saturated and unsaturated ceramides, ranging from Cer16:0 to Cer24:2. Data was acquired as previously described[17], and quantification was carried out by integrating peak areas for each individual analyte using Analyst 1.5.1 software. Recovery was assessed using internal standards, and values were normalized to protein content measured by a BCA assay.

Immunohistochemistry of mouse AAA

This was performed in a similar method to human AAA immunohistochemistry. Briefly, 5 μM cross sections of the paraffin embedded aortic tissue were cut, deparaffinized and antigen retrieval were performed. The aortic sections were blocked with 10% donkey serum and 0.3M Glycine in TBST buffer, treated with the primary antibodies in blocking buffer for overnight at 4 °C, washed in TBST. The primary antibodies used were Anti-Histone H3 (citrulline R2 + R8 + R17) (ab5103, Abcam); Rat anti Mouse F4/80, clone Cl:A3-1 (MCA497R, Bio-Rad); Rat anti Mouse Ly-6B.2 Alloantigen, clone 7/4 (MCA771G, Bio-Rad); and Monoclonal Anti-Actin, α-Smooth Muscle-Alkaline Phosphatase antibody, clone 1A4 (A5691, Sigma-Aldrich). For immunofluorescence, the secondary antibodies were Alexa Fluor 555 Donkey Anti-Rabbit IgG (A-31572, Invitrogen) and Alexa Fluor 488 Donkey Anti-Rat IgG (A-21208, Invitrogen), mounted with DAPI (H-1200, Vector Laboratories). Images were acquired on an inverted Zeiss LSM 700 and images were analyzed using ZEN 2012 software. For staining with chromogens, Anti-Rat IgG (whole molecule)–Alkaline Phosphatase antibody from Sigma-Aldrich (Cat. No. A8438) was used as secondary antibody and the stain was developed using SIGMAFAST™ Fast Red TR/ Naphthol AS-MX Tablets Sigma-Aldrich (Cat. No. F4523). Nuclei were visualized using hematoxylin stain and a permanent mounting medium with cover slip was applied before imaging on a Nikon light microscope. As a negative control, primary antibody was excluded in one out of the four AAA sections on a slide and staining was performed.

Western blotting

Standard Western blotting method was followed to examine the presence of Cit-H3 (Anti-Histone H3 (citrulline R2 + R8 + R17), ab5103, Abcam) in human or mouse aortic tissues. Briefly, aortic tissues were homogenized in RIPA buffer containing complete protease inhibitor (Sigma-Aldrich, St. Louis, MO) at 4 °C. The homogenate was centrifuged and total protein was estimated from the clear supernatant using BCA assay. A calculated volume of protein was treated with SDS-PAGE loading buffer containing β-marcaptoethanol before loading on to a 12% SDS-PAGE and blotted on a Nylon membrane. Subsequently, the blot was developed specifically as described by Abcam. As a positive control to Cit-H3, HL-60 lysate was used. To prepare HL-60 lysate, the cells were obtained from ATCC (Manassas, VA) and grown following the instruction provided by ATCC. More than 90% confluent cells were collected in PBS; lysed, centrifuged and clear supernatant was used for Western blotting.

Murine experimental AAA, adoptive transfer of neutrophils and drug treatments

All experimental procedures were performed according to the standard guideline for Animal Care and Use Committee at University of Virginia. Eight to ten weeks old male C57BL/6j

mice (The Jackson Laboratory, Bar Harbor, ME) and IL-1β KO mice (kindly provided by Gary Owens, University of Virginia) in C57BL/6 background were undergone elastase perfusion model of experimental murine AAA as described before[11]. At postoperative days 0, 3, 7 and 14, mice were euthanized under anesthesia by overdose and exsanguination. The abdominal aorta was dissected to expose the induced AAA and the largest diameter of the dilated section was measured. A short section of aorta just above the induced AAA was used and measured as self-control. The aortic diameter was measured using calibrated video microscopy with NIS-Elements D.3.10 software attached to the microscope (Nikon SMX-800, Melville, NY). Aortic diameters were determined in millimeters and the aortic dilation was calculated using (maximal AAA diameter − self-control aortic diameter)/ maximal AAA diameter × 100%. A dilation of ≥100% was considered to be positive for AAA.

Neutrophils from bone marrow of WT mice were isolated using mouse neutrophil isolation kit (Cat. No. 130-097-658) from Miltenyi Biotech (San Diego, CA). Immediately after the isolation, neutrophils were suspended in PBS and adoptively transferred to IL-1β KO mice via tail vein injection.

The PAD Inhibitor, Cl-amidine was obtained from EMD Millipore (Cat. No. 506282, Billerica, MA) and DNase I (Roche Diagnostics, Cat. No. 10104159001) was obtained from Fisher Scientific (Hampton, NH). Cl-amidine was solubilized in DMSO and diluted with PBS, whereas, DNase was directly dissolve in PBS before administrating the mice via intraperitoneal injections.

Flow cytometry quantification of immune cells in murine blood and AAA

After measuring the aortic diameter, elastase perfused aortas were collected, perfused with heparin-PBS solution to remove blood cells inside the aorta and digested to a cell suspension using enzymatic cocktail of collagenase type I (1000 U/ml), collagenase type XI (400 U/ml), Hyaluronidase type I-s (125 U/ml) and DNase (60 U/ml) as described before[18]. Immediately after the digestion, the cells were washed, blocked in flow cytometry buffer containing purified anti-mouse CD16/32, clone 93 (Biolegend, San Diego, CA) and stained with following fluorophore conjugated antibodies: PerCP/Cy5.5 anti-mouse CD19, clone 6D5; APC/Cy7 anti-mouse CD45, clone 30-F11; PE/Cy7 anti-mouse CD3ε, clone 145-2C11; Alexa Fluor 700 anti-mouse Ly-6G/Ly-6C (Gr-1) Antibody, clone RB6-8C5; Alexa Fluor 647 anti-mouse CD11c Antibody, clone N418 from Biolegend, San Diego, CA and F4/80 Rat Anti-Mouse mAb (clone BM8), Alexa Fluor 488 Conjugate, clone BM8, Invitrogen, (Carlsbad, CA). Red blood cells were lysed in 100 μl of blood and stained with the fluorescent conjugated antibodies. Following staining, the samples were run on a 16 color Flow cytometer machine Becton Dickinson LSRFortessa (equipped with laser lines 488nm, 405nm, 561nm, and 640nm) located in the Flow Cytometry Core Facility at University of Virginia. To count the number of cells, CountBright Absolute Counting Beads (Molecular Probes) were added to the cell suspension before flow cytometry. Fluorescent minus one (FMO) controls were used for each antibody in the experiment and dead cells were eliminated from analysis by staining with DAPI (4′, 6-diamidino-2-phenylindole, Sigma-Aldrich)

Statistical Analysis

GraphPad Prism 7 and Excel were used for data analysis and preparing graphs. In the multiple comparisons (one-way ANOVA), if a significant difference was found among the groups, pair of groups were compared using a post hoc test. Typically, a normality test (Shapiro-Wilk or D'Agostino & Pearson based on sample size) was performed in each group of data. If the data set passed a normality test (alpha=0.05), an F test was performed to compare variances between two groups. If the F test was not significantly different, unpaired Student's t-test was used. However, if F test was significantly different, unpaired t-test with Welch's correction was used. Differences were considered significant when P-value is <0.05.

RESULTS

IL-1β co-localizes with NETs in human AAA and blocking IL-1β binding to IL-1R inhibits NETosis in isolated neutrophils

Citrullination of histone H3 (Cit-H3) by peptidylarginine deiminase 4 (PAD4) causes condensation of nuclear chromatin and release of NETs, and inhibition of PAD4 activity leads to attenuation of NETosis. Therefore, presence of Cit-H3 in neutrophils is commonly used as marker of NETs[19]. Using confocal microscopy, we identified NETs as co-localized staining (yellow) of DNA (green) and either Cit-H3 (red) or neutrophil elastase (red) (Figure 1A). Interestingly, NETs were also found at the border of intima and media. Next, we examined if Cit-H3 could be quantified in homogenates from AAA tissues and plasma from AAA patients using Western blots. However, Cit-H3 was undetectable in AAA tissues or in the plasma (not shown).

Since IL-1β is crucial for experimental AAA formation[11], we examined if IL-1β concentrates at the site of NETs. Staining of human AAA adjacent sections with Cit-H3 and IL-1β antibodies revealed co-localization of high concentration of IL-1β with NETs (Figure 1B). Next, to determine if IL-1β binding to neutrophils is required for NETosis, neutrophils were isolated from healthy human volunteers and treated with recombinant human IL-1β. The isolated neutrophils were >95% live and >90% pure as determined on a flow cytometer (Supplemental Figure I). As described previously by Mitroulis et al.[6], IL-1β treatment induced NETosis which was confirmed by co-localization of DNA with neutrophil elastase or Cit-H3 using confocal microscopy (Supplemental Figure II). Total DNA positive area and total nuclear area were determined using ImageJ, and NETosis was calculated as the ratio of DNA positive area to nuclear area (Supplemental Figure III). IL-1β induced NETosis in a dose-dependent manner and pretreatment of neutrophils with IL-1RA significantly decreased NETosis (Figure 1C and D). This result not only supports the finding of Mitroulis et al. which demonstrates 'IL-1RA inhibits IL-1β-induced NETosis' (%NETosis was determined by counting the number of cells releasing NETs), but also validates our new method of NET quantification *in vitro*. Furthermore, this result was confirmed by quantification of PicoGreen staining of dsDNA released to culture supernatant after induction of NETosis (Supplemental Figure IV)[15, 16]. Altogether, these results suggest that IL-1β binding to IL-1R on neutrophils is crucial for induction of NETosis.

IL-1β triggers ceramide synthesis in human neutrophils and inhibition of IL-1β binding or ceramide synthesis attenuates NETosis

CerS6 is localized in perinuclear region and synthesizes long-chain ceramides such as C14- and C16-ceramides[13]. Therefore, we tested the hypothesis that IL-1β-induced NETosis requires ceramide synthesis. First, we examined if IL-1β treatment affects CerS6 cellular localization using immunocytochemistry. Neutrophils isolated form human blood were left untreated or pre-treated with IL-1RA before stimulating IL-1β. IL-1β treatment promoted nuclear localization of CerS6 in intact neutrophils, which was prevented in presence of IL-1RA (Figure 2A). To quantify IL-1β-induced ceramide synthesis, human neutrophils were treated with a lower concentration of IL-1β (to prevent NETosis and, thereby prevent the loss of intracellular ceramides) and intracellular ceramides were extracted and quantified using LS-MS/MS. IL-1β treatment increased the levels of both short-chain and long-chain ceramides, specifically the levels of highly abundant Cer 16:0 and Cer 24:1 compared to untreated neutrophils (Figure 2B). Next, to examine if inhibition of IL-1β signaling prevents ceramide synthesis, intracellular ceramide levels were quantified in neutrophils that were pre-treated with IL-1RA followed by IL-1β treatment. The results revealed that IL-1RA attenuated synthesis of Cer 16:0 (Figure 2C), whereas, no differences were found in the level of Cer 24:1 (not shown).

To examine if *de novo* ceramide synthesis pathway is induced by IL-1β treatment, neutrophils were pretreated with either Myriocin, an inhibitor of serine palmitoyltransferase or Fumonisin B1, an inhibitor of ceramide synthase, and then treated with IL-1β. Interestingly, pre-treatment with Fumonisin B1, but not Myriocin, significantly decreased IL-1β-induced Cer 16:0 synthesis (Figure 2C). In this line, Fumonisin B1 attenuated IL-1β-induced NETosis (Figure 2D).

Since increased IL-1β synthesis has been reported in human AAA tissues[11], we examined if the levels of ceramides are also increased in human AAA tissues. Ceramides were extracted from homogenates of normal aorta and AAA tissues, and analyzed by mass spectrometry. The results revealed a significant increase of Cer 16:0 in AAA tissues, compared to normal aorta (Supplemental Figure V).

Altogether, these results suggest that IL-1β promotes ceramide biosynthesis in human neutrophils *via* the *de novo* pathway and long-chain ceramide synthesis is significantly increased in human AAA tissues.

NETs are formed in early stages of murine experimental AAA

To determine if NETs are present in experimental murine AAA, the abdominal aortas of C57BL/6 (WT) mice underwent elastase perfusion[11], were harvested at days 0, 3, 7 or 14, and stained for NETs, which were identified by neutrophil (Ly6B.2) + Cit-H3 + DNA co-localized staining. Maximal staining for Cit-H3 was found at day 3 (Figure 3A, Supplemental Figure VI). Cit-H3, but not neutrophil elastase staining, was strongly co-localized with DNA and neutrophil staining, suggesting a high rate of NETosis at day 3 after elastase perfusion (Supplemental Figure VI and VII). To further confirm presence of NETs, high-resolution 3-dimensional confocal images were acquired which demonstrated the

presence of NETs in the intima of aortas harvested at day 3 after elastase perfusion (Figure 3B). To quantify NETosis, total protein from abdominal aortas were collected at day 0, 3, 7 and 14 after elastase perfusion and separated on a SDS-PAGE and Western blotting was performed using Cit-H3. The Cit-H3 level was significantly higher in aortas at day 3 confirming high rate of NETosis at day 3 compared to day 0, however, no significant differences were found in Cit-H3 levels of days 7 and 14 (Figure 3C). Altogether, these results suggest that neutrophils undergo NETosis at an early stage of induction of experimental AAA.

IL-1β expression in neutrophils is required for AAA formation in mice

Infiltration of immune cells, such as neutrophils[4], B cells[20] and T cells[21] are required for AAA formation. Since neutrophil infiltration and NETosis occur at an early stage of AAA formation, we hypothesized that in the absence of IL-1β, infiltration of neutrophils and other immune cells is repressed, leading to protection from AAA. To test this hypothesis, we induced AAA in WT and IL-1β KO mice (Supplemental Figure VIII), examined AAA formation and, using flow cytometry, counted the number of circulating and aortic infiltrated immune cells at day 7, which is considered an early phase of AAA formation. As expected, the increase in AAA diameter was significantly lower in the IL-1β KO mice compared to WT mice (Figure 4A). Interestingly, although the number of circulating neutrophils (Gr1+ cells) was similar in WT and IL-1β KO mice, the number of aortic infiltrated neutrophil was significantly lower in the KO mice. Moreover, the number of circulating hematopoietic cells (CD45+), including B cells (CD19+) was significantly higher in the KO animals but lower in the AAA of the IL-1β KO mice (Figure 4B). These results suggest that IL-1β is crucial for infiltration of immune cells to the site of AAA.

Next, to determine the role of neutrophil IL-1β in aneurysm formation, AAA was induced *via* elastase perfusion in IL-1β KO mice, followed by adoptive transfer of neutrophils isolated from bone marrow of WT mice. First, we examined the survival of WT neutrophils in the IL-1β KO mice by injecting 5×10^6 WT neutrophils (isolated from bone marrow of WT mice) into IL-1β KO mice *via* tail vein and inducing AAA *via* elastase perfusion. PBS was injected as a control. Since neutrophils were the only source of IL-1β in the IL-1β KO mice, presence of IL-1β+ neutrophils was determined by real-time RT-PCR of blood, which was drawn on days 3 and 7 after the injection. IL-1β expression was detected until day 3 in the WT neutrophil transferred mice, which was undetectable until day 7 (Supplemental Figure IXA). Therefore, 5×10^6 WT neutrophils were transferred to these mice on day 7 and AAA formation was determined on day 14 by video micrometry. No significant differences were found in AAA formation (56.9±8.1% and 52.8±7.3%, vehicle vs neutrophil adoptive transfer) (Supplemental Figure IXB).

Next, higher doses of WT neutrophils were injected to the IL-1β KO mice and AAA was induced. 10×10^6 neutrophils were injected consecutively on days 0 and 1 (total 20×10^6) or consecutively on days 0, 1, 2 and 3 (total 40×10^6). As a negative control, saline was injected to IL-1β KO mice. Fourteen days after AAA induction, AAA size was determined using video micrometry. The results revealed a significant increase in AAA size in the mice receiving 40×10^6 total neutrophils compared to the control mice (44.2±4.9, 63.1±21.1 and

97.3±15.9% in IL-1β KO injected with PBS, 20×10^6 and 40×10^6 WT neutrophils, respectively) (Figure 4C). There was weak evidence of elastin degradation and decreased staining of smooth muscle alpha-actin in the AAA of 40×10^6 neutrophil-transferred mice (Figure 4D). Since the aortas were harvested at day 14, no significant difference in Cit-H3 level was found in animals receiving saline and 40×10^6 WT neutrophils (not shown). These results suggest that neutrophil derived IL-1β induces aortic degradation and promotes AAA formation.

Cl-amidine, not DNase attenuates AAA formation in mice

Two methods of suppressing NETosis-mediated inflammation have been described, i.e. Cl-amidine and deoxyribonuclease (DNase) treatment. Cl-amidine suppresses NETosis by inhibiting the enzyme PAD4, whereas, DNase digests the DNA in the NETs. Both Cl-amidine and DNase are known to protect mice from atherosclerosis by inhibiting NETosis[19, 22]. To determine if either of these drugs can attenuate experimental AAA formation, we injected WT mice with two different concentrations of Cl-amidine or DNase and induced AAA *via* elastase perfusion method. Cl-amidine was injected once per day at 10 or 20 mg/kg, whereas DNase was injected twice per day (because of the shorter half-life) at 2.5 or 7.5 mg/kg (Figure 5 A and B). As a control, saline was injected to WT mice. On day 14 of elastase perfusion, injection of Cl-amidine at a higher dose (20 mg/kg) had attenuated AAA formation (126.5±20.9, 106.4±21 and 89.2±18.7% dilatation in mice receiving saline, 10 mg/kg and 20 mg/kg of Cl-amidine) (Figure 5A). However, DNase injections did not affect AAA formation (109.3±17.5, 116.4±30.7 and 109.4±32.1% dilatation in mice receiving saline, 2.5 mg/kg and 7.5 mg/kg of DNase) (Figure 5B). Immunohistology on cross-sections of AAA tissues provided weak evidence of reduced elastin degradation and macrophage staining in the aortas in Cl-amidine injected mice, confirming attenuation of AAA formation (Figure 5C). Altogether, our results indicate that the NETosis inhibitor Cl-amidine improves aortic health and attenuates elastase-induced AAA formation in mice.

DISCUSSION

In infections, NETosis not only promotes containment of pathogens, but also the killing of pathogens *via* histones and enzymes, such as neutrophil elastase and myeloperoxidase, which decorate NET fibers[23]. While NETosis is beneficial for clearance of pathogens, induction of NETosis in sterile inflammation seems to be deleterious for many chronic diseases, including atherosclerosis[5], gout[6] and systemic inflammatory response syndrome (SIRS) [7]. For example, once released, histones act as damage-associated molecular pattern molecules and activate Toll-like receptors leading to systemic inflammation[24]. Megens et al. have shown that 57% of the apolipoprotein E KO mice on Western diet for 4–6 weeks displayed NETs in atherosclerotic plaques as opposed to none in mice on regular chow diet[5]. We have previously reported that IL-1β expression is significantly higher in human AAAs and inhibition of IL-1β signaling *via* IL-1RA strongly attenuates murine experimental AAA formation[11]. Here we demonstrated that IL-1RA can potentially inhibit NETosis in isolated human neutrophils. In support of our study, Mitroulis et al. have reported that synovial fluids from inflamed joints of gout patients induced NETosis in healthy neutrophils, which was inhibited by IL-1RA treatment[6]. Our results demonstrate that NETs are present in human

AAAs and are decorated at least with Cit-H3 and neutrophil elastase. Extracellular histones have been shown to have deleterious effects by activating platelets causing thrombocytopenia[25], and promoting cell death via activation of Toll-like receptors 2 and 4[26]. Therefore, NETs in AAAs may cause a sterile inflammatory microenvironment. In support of this hypothesis, we found IL-1β in NETs of human AAAs.

Multiple mechanisms have been proposed to describe how NETs are formed, such as, activation of NADPH oxidase [27] or histone deimination by peptidylarginine deiminase PAD4 [19]. Involvement of ceramides in NETosis has not been examined. Ceramides are precursors of sphingolipids in cells and critically involved in apoptosis[28]. Synthesis of both the cytoplasmic and nuclear ceramide increase during apoptosis. Cellular ceramide synthesis is regulated by sphingomyelinases (salvage pathway) and/or serine palmitoyltransferase and ceramide synthases (*de novo* pathway). Our results suggest that IL-1β-induced ceramide synthesis triggers NETosis, which can be attenuated by inhibition of IL-1β signaling (IL-1RA treatment) or inhibition of ceramide synthases (Fumonisin B1 treatment). Specifically, synthesis of Cer 16:0 was attenuated by both IL-1RA and Fumonisin B1. Seumois et al. have reported that *de novo* synthesis of Cer 16:0 is significantly increased in cultured human neutrophils and leads to spontaneous apoptosis[29]. Although further experimentation is required, our results fit into a model that IL-1β induces nuclear translocation of CerS6 leading to nuclear Cer 16:0 synthesis, which permeabilizes nuclear membrane and triggers NETosis.

Using an experimental model of murine AAA, we examined if IL-1β-induced NETosis can promote AAA formation. We found that NETs appeared in aortas as early as day 3 of AAA induction. Presence of NETs in mouse AAAs was confirmed by the co-localization of 3 markers: DNA, Cit-H3 and Ly6B.2 (neutrophil). In accordance with our previous report, genetically disrupting IL-1β signaling (IL-1β KO mice) attenuated AAA formation at an early stage. Furthermore, the protection was associated with lower immune cell infiltration, including neutrophils. Since IL-1β produced by neutrophils can also induce NETosis, we adoptively transferred WT neutrophils to IL-1β KO mice and induced AAA. WT neutrophils promoted AAA formation in the IL-1β KO mice with increased aortic damage. It can be hypothesized that IL-1β released from WT neutrophils promoted infiltration of inflammatory cells including IL-1β deficient neutrophils leading to release of NETs and AAA formation.

Furthermore, in WT mice, we detected increased level of Cit-H3 at day 3 after elastase perfusion. In the neutrophil adoptive transfer experiment, aortas were collected at day 14 after elastase perfusion to determine AAA formation. At day 14, neutrophils do not represent a major cellular population in AAAs because of lymphocyte and macrophage infiltration, and massive aortic remodeling. Moreover, IL-1β produced by WT neutrophils can attract other inflammatory cells to promote aneurysm formation irrespective of NETosis. Therefore, we examined the effect of Cl-amidine treatment (to decrease PAD4 activity, decrease H3 citrullination and NETosis) or DNase treatment (to digest NETs and decrease inflammation). As far as atherosclerosis is concerned, inhibition of NETosis by Cl-amidine treatment[19], or degrading NETs by DNase treatment [22] decreased atherosclerosis. Our results suggest that, Cl-amidine, but not DNase, attenuates AAA formation in mice.

There are several limitations to the current study. First, Yan et al. showed that DNase treatment attenuated aneurysm formation in an elastase model of mouse AAA[8]. We tried two different doses of DNase administration, and did not find any difference in AAA formation compared to the untreated mice. The discrepancy in the results may be explained by difference in the sources of DNase. Second, our study suggests NETs occupy a relatively small area in human AAA tissue. Therefore, it is possible that the ceramides we quantified from the whole AAA tissue are primarily from smooth muscle cells and other adventitial cells. Despite this fact, Cer 16:0 level was higher in AAA tissue compared to the normal aortic tissues. Third, Myriocin did not inhibit ceramide synthesis. Myriocin is a strong inhibitor of serine palmitoyltransferase. In the *de novo* ceramide biosynthesis pathway, serine palmitoyltransferase is upstream of ceramide synthases. In our study, we did not find decrease in ceramide levels after Myriocin treatment. This may be because of the low concentration of Myriocin used in this study. We found that Myriocin at 20 μM concentration significantly attenuated basal level synthesis of Cer 4:0 to Cer 24:1 in cultured human neutrophils (not shown). Therefore, a lower concentration, i.e. 5 μM was selected for the current study. Fourth, in the figures 4 and 5, video micrometry determination of AAA demonstrated larger AAAs in the WT-neutrophil transferred IL-1β KO mice and smaller AAAs in the Cl-amidine-treated WT mice. Number of mice used in these experiments was 9–11. However, 3–4 mice per group were used in the immunohistology analyses to determine AAA pathology in the figures 4D and 5C, which increases the probability for a beta error.

In summary, this study clearly demonstrates the presence of NETs in human and experimental murine AAAs. Neutrophils undergo NETosis in the early phase of AAA growth in mice. Formation of AAAs in mice requires IL-1β in neutrophils. Importantly, our *in vitro* studies demonstrated that IL-1β triggers ceramide synthesis in human neutrophils and inhibition of IL-1β binding to IL-1R or inhibition of ceramide synthesis attenuates NETosis. In a separate experiment, we demonstrated that the NETosis inhibitor Cl-amidine attenuates AAA formation. Both of these studies fit to a model in which IL-1β triggers ceramide synthesis in aortic infiltrated neutrophils and induces NETosis, which further leads to AAA formation (Supplemental Figure X). Thus, our study suggests inhibition of NETosis is a possible treatment strategy against AAAs.

Supplementary Material

Refer to Web version on PubMed Central for supplementary material.

Acknowledgments

We acknowledge the assistance of Flow Cytometry Core Facility, Advanced Microscopy Facility and Research Histology Core at University of Virginia. AKM and GRU conceived the project, designed experiments, and wrote the manuscript. AKM, MS, JDP, NP, GS and VS performed experiments and/or interpreted data. VEL provided Institutional Review Board protocol for collection of human blood. NL and GA provided reagents and advice.

SOURCES OF FUNDING

This work was supported by NIH 5R01HL124131 (G.R.U), National Scientist Development Grant 14SDG20380044 from the American Heart Association (A.K.M.), NIH R01 1R01HL126668 (G.A.), NIH R01

DK096076 and a Grant in Aid from the American Heart Association (N.L.). V.S. was supported by an AHA Predoctoral Grant 15PRE255600036 and Pharmacological Sciences Training Grant T32-GM007055-40.

Non standard abbreviations and acronyms

AAA	Abdominal aortic aneurysm
NET	Neutrophil Extracellular Trap
NETosis	Formation of Neutrophil Extracellular Trap
Cit-H3	Citrullinated histone H3
IL-1RA	IL-1 Receptor Antagonist

References

1. Forsdahl SH, Singh K, Solberg S, Jacobsen BK. Risk factors for abdominal aortic aneurysms: A 7-year prospective study: The tromso study, 1994–2001. Circulation. 2009; 119:2202–2208. [PubMed: 19364978]
2. Rizas KD, Ippagunta N, Tilson MD 3rd. Immune cells and molecular mediators in the pathogenesis of the abdominal aortic aneurysm. Cardiology in review. 2009; 17:201–210. [PubMed: 19690470]
3. Dale MA, Ruhlman MK, Baxter BT. Inflammatory cell phenotypes in aaas: Their role and potential as targets for therapy. Arteriosclerosis, thrombosis, and vascular biology. 2015; 35:1746–1755.
4. Eliason JL, Hannawa KK, Ailawadi G, Sinha I, Ford JW, Deogracias MP, Roelofs KJ, Woodrum DT, Ennis TL, Henke PK, Stanley JC, Thompson RW, Upchurch GR Jr. Neutrophil depletion inhibits experimental abdominal aortic aneurysm formation. Circulation. 2005; 112:232–240. [PubMed: 16009808]
5. Megens RT, Vijayan S, Lievens D, Doring Y, van Zandvoort MA, Grommes J, Weber C, Soehnlein O. Presence of luminal neutrophil extracellular traps in atherosclerosis. Thrombosis and haemostasis. 2012; 107:597–598. [PubMed: 22318427]
6. Mitroulis I, Kambas K, Chrysanthopoulou A, Skendros P, Apostolidou E, Kourtzelis I, Drosos GI, Boumpas DT, Ritis K. Neutrophil extracellular trap formation is associated with il-1beta and autophagy-related signaling in gout. PloS one. 2011; 6:e29318. [PubMed: 22195044]
7. Keshari RS, Jyoti A, Dubey M, Kothari N, Kohli M, Bogra J, Barthwal MK, Dikshit M. Cytokines induced neutrophil extracellular traps formation: Implication for the inflammatory disease condition. PloS one. 2012; 7:e48111. [PubMed: 23110185]
8. Yan H, Zhou HF, Akk A, Hu Y, Springer LE, Ennis TL, Pham CT. Neutrophil proteases promote experimental abdominal aortic aneurysm via extracellular trap release and plasmacytoid dendritic cell activation. Arteriosclerosis, thrombosis, and vascular biology. 2016; 36:1660–1669.
9. Tavora FR, Ripple M, Li L, Burke AP. Monocytes and neutrophils expressing myeloperoxidase occur in fibrous caps and thrombi in unstable coronary plaques. BMC Cardiovasc Disord. 2009; 9:27. [PubMed: 19549340]
10. Mohanan S, Horibata S, McElwee JL, Dannenberg AJ, Coonrod SA. Identification of macrophage extracellular trap-like structures in mammary gland adipose tissue: A preliminary study. Front Immunol. 2013; 4:67. [PubMed: 23508122]
11. Johnston WF, Salmon M, Su G, Lu G, Stone ML, Zhao Y, Owens GK, Upchurch GR Jr, Ailawadi G. Genetic and pharmacologic disruption of interleukin-1beta signaling inhibits experimental aortic aneurysm formation. Arteriosclerosis, thrombosis, and vascular biology. 2013; 33:294–304.
12. Tirodkar TS, Voelkel-Johnson C. Sphingolipids in apoptosis. Experimental oncology. 2012; 34:231–242. [PubMed: 23070008]
13. White-Gilbertson S, Mullen T, Senkal C, Lu P, Ogretmen B, Obeid L, Voelkel-Johnson C. Ceramide synthase 6 modulates trail sensitivity and nuclear translocation of active caspase-3 in colon cancer cells. Oncogene. 2009; 28:1132–1141. [PubMed: 19137010]

14. Davis CN, Tabarean I, Gaidarova S, Behrens MM, Bartfai T. Il-1beta induces a myd88-dependent and ceramide-mediated activation of src in anterior hypothalamic neurons. Journal of neurochemistry. 2006; 98:1379–1389. [PubMed: 16771830]
15. Liu S, Su X, Pan P, Zhang L, Hu Y, Tan H, Wu D, Liu B, Li H, Li H, Li Y, Dai M, Li Y, Hu C, Tsung A. Neutrophil extracellular traps are indirectly triggered by lipopolysaccharide and contribute to acute lung injury. Sci Rep. 2016; 6:37252. [PubMed: 27849031]
16. Tanaka K, Koike Y, Shimura T, Okigami M, Ide S, Toiyama Y, Okugawa Y, Inoue Y, Araki T, Uchida K, Mohri Y, Mizoguchi A, Kusunoki M. In vivo characterization of neutrophil extracellular traps in various organs of a murine sepsis model. PloS one. 2014; 9:e111888. [PubMed: 25372699]
17. Patel SA, Hoehn KL, Lawrence RT, Sawbridge L, Talbot NA, Tomsig JL, Turner N, Cooney GJ, Whitehead JP, Kraegen EW, Cleasby ME. Overexpression of the adiponectin receptor adipor1 in rat skeletal muscle amplifies local insulin sensitivity. Endocrinology. 2012; 153:5231–5246. [PubMed: 22989629]
18. Meher AK, Johnston WF, Lu G, Pope NH, Bhamidipati CM, Harmon DB, Su G, Zhao Y, McNamara CA, Upchurch GR Jr, Ailawadi G. B2 cells suppress experimental abdominal aortic aneurysms. The American journal of pathology. 2014; 184:3130–3141. [PubMed: 25194661]
19. Knight JS, Luo W, O'Dell AA, Yalavarthi S, Zhao W, Subramanian V, Guo C, Grenn RC, Thompson PR, Eitzman DT, Kaplan MJ. Peptidylarginine deiminase inhibition reduces vascular damage and modulates innate immune responses in murine models of atherosclerosis. Circulation research. 2014; 114:947–956. [PubMed: 24425713]
20. Schaheen B, Downs EA, Serbulea V, Almenara CC, Spinosa M, Su G, Zhao Y, Srikakulapu P, Butts C, McNamara CA, Leitinger N, Upchurch GR Jr, Meher AK, Ailawadi G. B-cell depletion promotes aortic infiltration of immunosuppressive cells and is protective of experimental aortic aneurysm. Arteriosclerosis, thrombosis, and vascular biology. 2016; 36:2191–2202.
21. Xiong W, Zhao Y, Prall A, Greiner TC, Baxter BT. Key roles of cd4+ t cells and ifn-gamma in the development of abdominal aortic aneurysms in a murine model. Journal of immunology. 2004; 172:2607–2612.
22. Warnatsch A, Ioannou M, Wang Q, Papayannopoulos V. Inflammation. Neutrophil extracellular traps license macrophages for cytokine production in atherosclerosis. Science. 2015; 349:316–320. [PubMed: 26185250]
23. Hirsch JG. Bactericidal action of histone. The Journal of experimental medicine. 1958; 108:925–944. [PubMed: 13598820]
24. Chen R, Kang R, Fan XG, Tang D. Release and activity of histone in diseases. Cell death & disease. 2014; 5:e1370. [PubMed: 25118930]
25. Fuchs TA, Bhandari AA, Wagner DD. Histones induce rapid and profound thrombocytopenia in mice. Blood. 2011; 118:3708–3714. [PubMed: 21700775]
26. Xu J, Zhang X, Monestier M, Esmon NL, Esmon CT. Extracellular histones are mediators of death through tlr2 and tlr4 in mouse fatal liver injury. Journal of immunology. 2011; 187:2626–2631.
27. Munoz-Caro T, Lendner M, Daugschies A, Hermosilla C, Taubert A. Nadph oxidase, mpo, ne, erk1/2, p38 mapk and ca2+ influx are essential for cryptosporidium parvum-induced net formation. Developmental and comparative immunology. 2015; 52:245–254. [PubMed: 26026247]
28. Chaurasia B, Summers SA. Ceramides - lipotoxic inducers of metabolic disorders. Trends in endocrinology and metabolism: TEM. 2015; 26:538–550. [PubMed: 26412155]
29. Seumois G, Fillet M, Gillet L, Faccinetto C, Desmet C, Francois C, Dewals B, Oury C, Vanderplasschen A, Lekeux P, Bureau F. De novo c16- and c24-ceramide generation contributes to spontaneous neutrophil apoptosis. Journal of leukocyte biology. 2007; 81:1477–1486. [PubMed: 17329567]

HIGHLIGHTS

- NETs are present in human and murine AAAs.
- IL-1β incudes ceramide synthesis in human neutrophils and inhibition of ceramide synthesis attenuates IL-1β-induced NETosis.
- Neutrophil-derived IL-1β promotes the formation of murine AAAs.
- NETosis inhibitor Cl-amidine attenuates murine AAA formation.

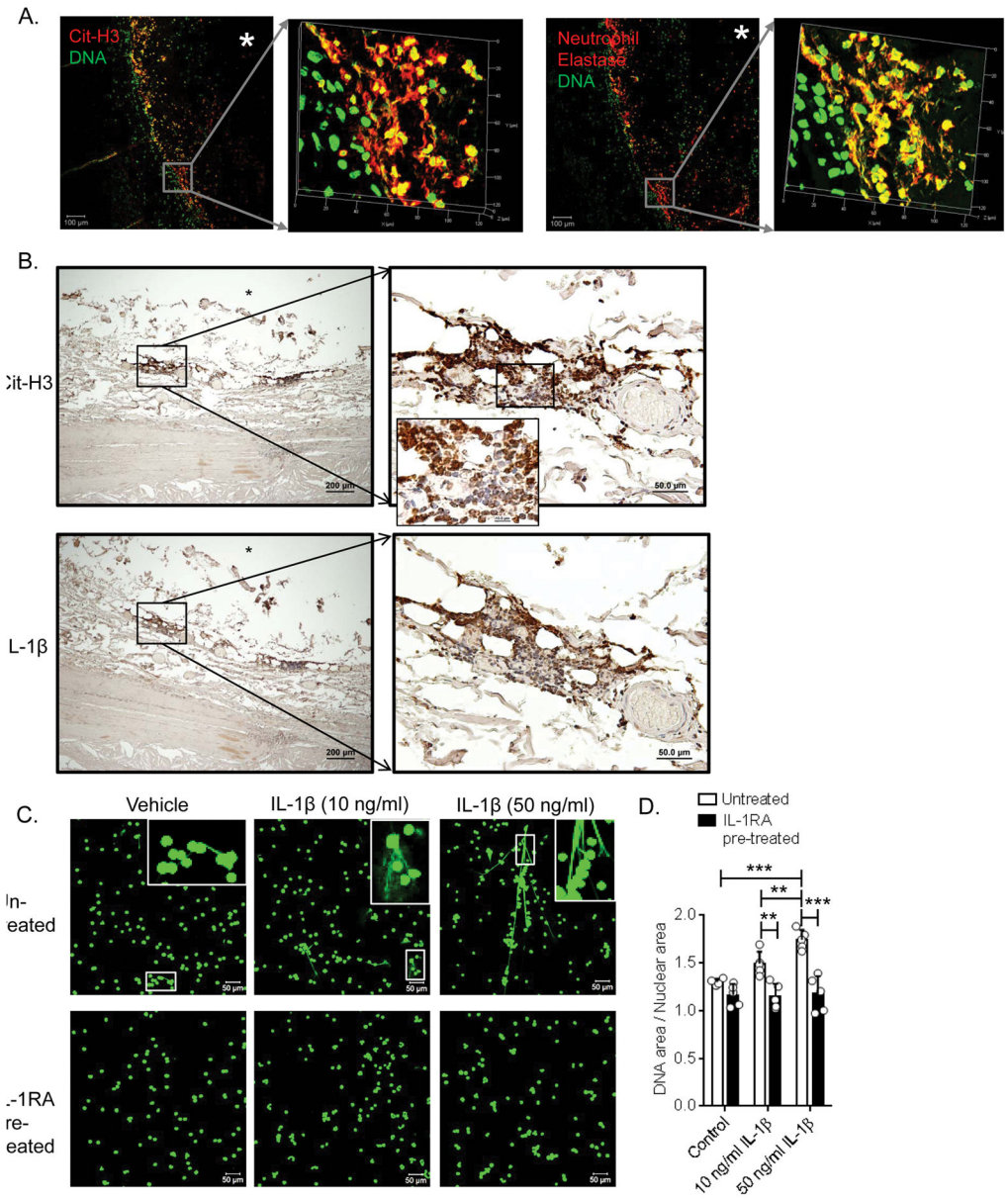

Figure 1. Identification and co-localization of IL-1β and NETs in human AAA, and induction of NETosis by IL-1β in human neutrophils

(**A**), Confocal image showing NETs (yellow) identified as co-localization of DNA (green, YO-PRO-1) and neutrophil elastase (red) or Cit-H3 (red). Scale, 100 μm and "*" indicates lumen. Right panel: 3D representation of a small segment from left panel. (**B**), Top panel Cit-H3 and bottom panel, IL-1β staining of consecutive sections of human AAA. "*" indicates lumen. (**C**), Neutrophils isolated from human blood was left untreated or pretreated with 100 ng/ml of IL-1RA for 30 min and then treated with 10 or 50 ng/ml of IL-1β for 3 hours. The cells were fixed, permeabilized, stained with the DNA dye DAPI (green) and images were acquired on a confocal microscope. Insets are enlarged images showing NETs. (**D**), NETosis was quantified as ratio of DNA+ area/ Nuclear area using ImageJ. Values are expressed as means±SD and n=5. '**' and "***" indicate P<0.01 and 0.001, respectively,

determined by two-way ANOVA followed by comparison between two groups, which was determined by a normality test (Shapiro-Wilk, alpha=0.05) followed by unpaired t-test with Welch's correction (F test to compare variances was not significantly different).

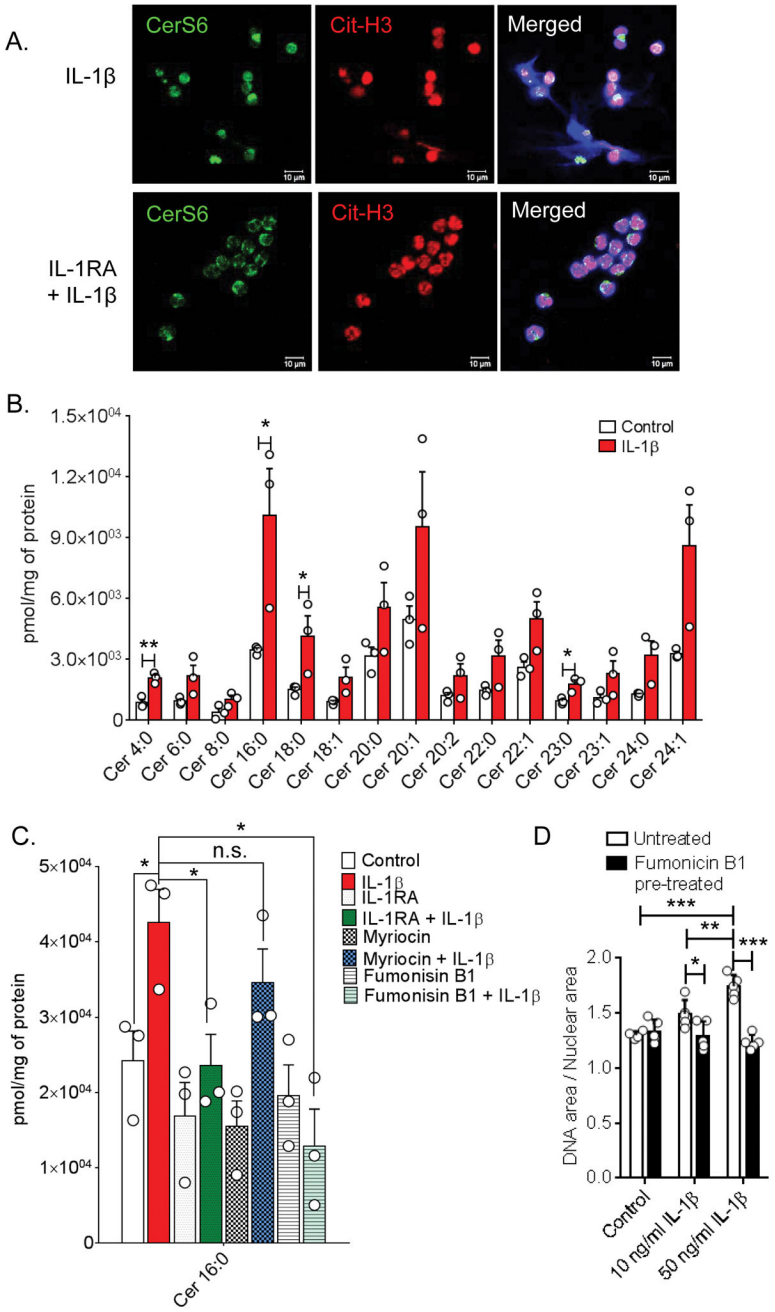

Figure 2. IL-1β induces nuclear translocation of CerS6 and ceramide synthesis, which are attenuated by IL-1RA or Fumonisin B1

(**A**), Human neutrophils were seeded on polylysine-coated glass cover glasses, left untreated or pretreated with 100 ng/ml of IL-1RA and NETosis was induced with 50 ng/ml of IL-1β. The cells were fixed, permeabilized and stained with DNA dye DAPI (blue), Cit-H3 (red) and ceramide synthase 6 (green, CerS6), and images were acquired on a confocal microscope. Scale bar, 10 μm. (**B**), Human neutrophils were treated with vehicle (Control) or 10 ng/ml of IL-1β for 5 hours. Ceramides were extracted and quantified using LC-MS/MS. Values are expressed as means±SD and n=3. (**C**), Human neutrophils were pretreated with

vehicle (Control), IL-1RA (100 ng/ml), Myriocin (5 μM) or Fumonicin B1 (10 μM) for 30 min and then either left untreated or treated with 10 ng/ml of IL-1β for 5 hours, and ceramides were quantified using LC-MS/MS. Values are expressed as means±SD and n=3. (**D**), Human neutrophils were seed on polylysine coted cover glasses and pretreated with vehicle (Control) or Fumonicin B1 (10 μM) for 30 min and then either left untreated or treated with 50 ng/ml of IL-1β for 3 hours. The cells were stained for DNA (DAPI) and NETosis was quantified as ratio of DNA+ area/ Nuclear area using ImageJ. Values are expressed as means±SD and n=5. '**' and "***" indicates P<0.01 and 0.001, respectively, determined by determined by two-way ANOVA followed by comparison between two groups, which was determined by a normality test (Shapiro-Wilk, alpha=0.05) followed by unpaired t-test with Welch's correction (F test to compare variances was not significantly different).

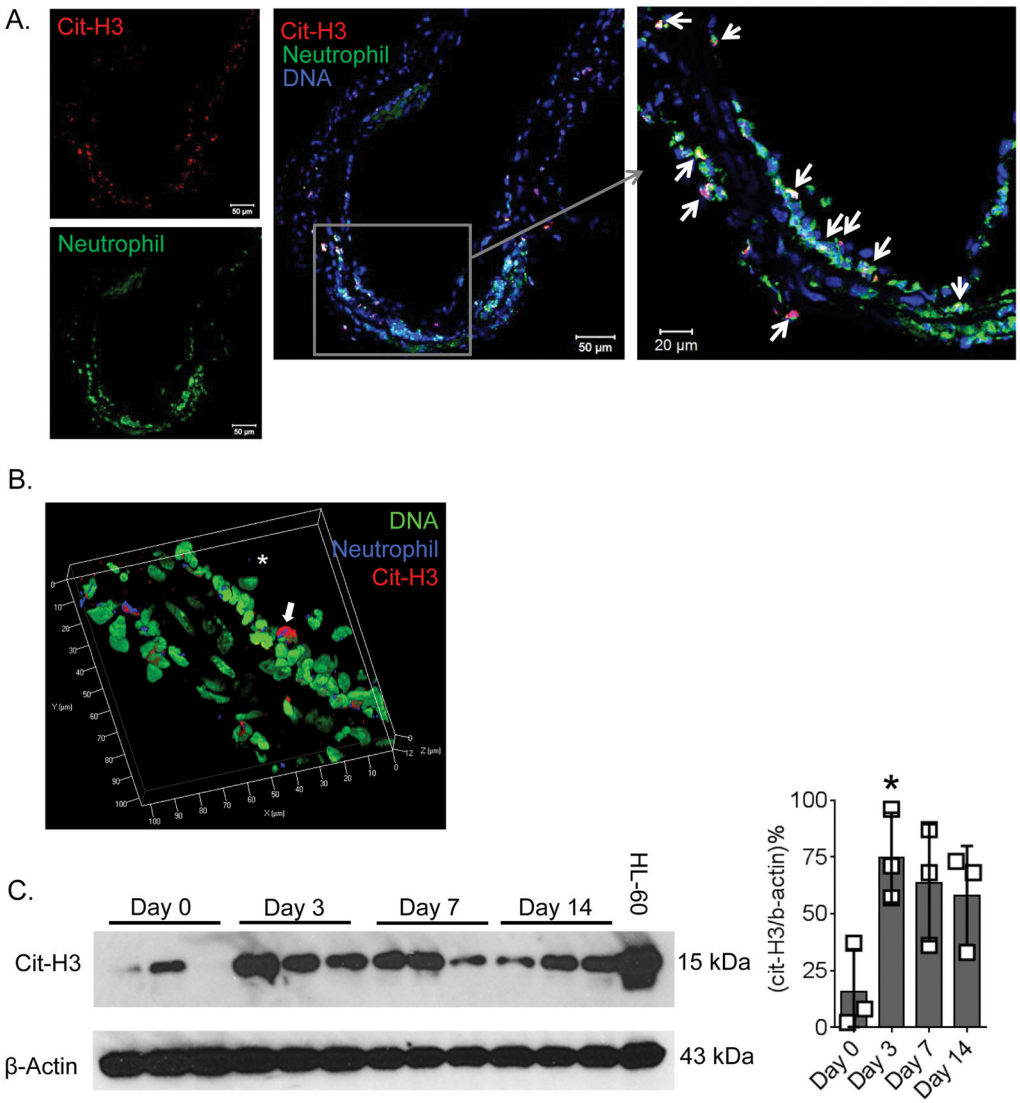

Figure 3. NETs are formed in early stages of experimental AAA

AAA was induced in wild-type mice via elastase perfusion and aortas were harvested at day 3. (**A**), Aortic sections were stained with Cit-H3 (red), Ly6B.2 (green, neutrophil) and DAPI (blue, DNA). White arrows indicate colocalization of Cit-H3, neutrophil and DNA demonstrating presence of NETs. (**B**), Aortic sections were stained with Cit-H3 (red), Ly6B.2 (blue, neutrophil) and DAPI (green, DNA), high resolution 2D images were acquired on a confocal microscope and combined to generate the 3D image. Arrow indicates NETs formed at the luminal site of the aorta. (**C**), Left panel, Abdominal aortas of WT mice were harvested at days 0, 3, 7 and 14 after induction of AAA and the aorta homogenates were run on a 12% SDS-PAGE and Western blotting was performed against Cit-H3 and β-actin. HL-60 cell lysate was used as a positive control for Cit-H3. Right panel, ratio of band intensity of Cit-H3 and β-actin. Values are expressed as means±SD and n=3/group. '*' indicates $P<0.05$, determined by 1-way ANOVA with Dunnett's multiple comparisons test.

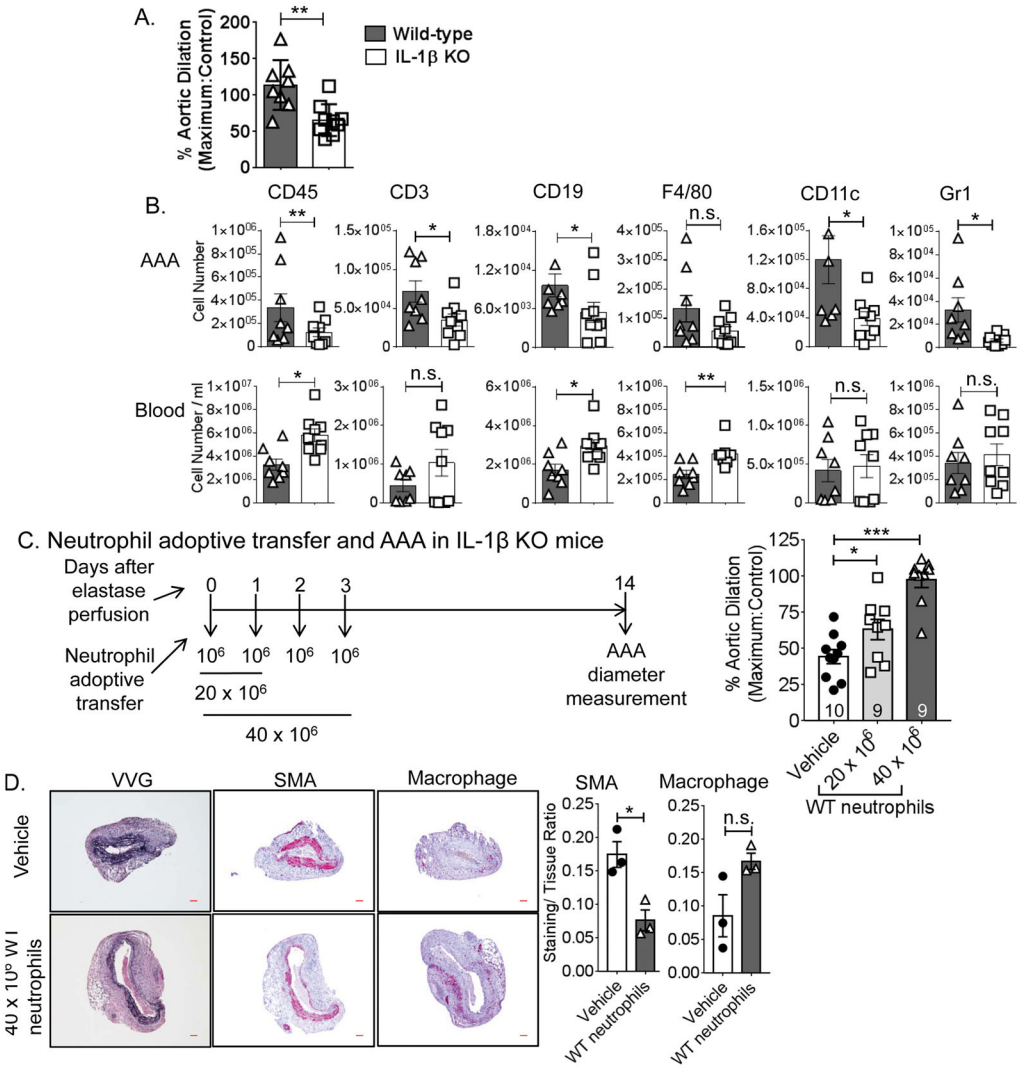

Figure 4. IL-1β KO mice demonstrate decreased AAA formation and immune cell infiltration to aorta, which are reversed by adoptive transfer of WT neutrophils

(**A**), AAA was induced in WT and IL-1β KO mice via elastase perfusion and aortic dilation was determined after 7 days. Values are expressed as means±SE and n= 8–9. (**B**), Immune cells were quantified in aortas and blood of WT and IL-1β KO mice by using Flow cytometry. Values are expressed as means+SE and n= 8–9. (**C**), WT neutrophils at two different doses were adoptively transferred to IL-1β KO mice and aortic dilation was determined 14 days after elastase perfusion. As a control, saline (Vehicle) was injected to IL-1β KO mice. Values are expressed as means±SE. The number of mice used in each group is indicated within the bars. (**D**), AAA pathology from the vehicle or neutrophil adoptive transferred mice was determined by Verhoeff-Van Gieson (VVG), smooth muscle α-actin (SMA, red) and macrophage (F 4/80, red) staining. Scale bar, 100 μm. Right panels, quantification of SMA and macrophage staining area, n=3/group. Significant difference between the two groups was determined by a normality test (D'Agostino & Pearson, alpha=0.05, for **A**, **B** and **C**; Shapiro-Wilk, alpha=0.05, for **D**) followed by unpaired t-test with Welch's correction (F test to compare variances was not significantly different). '*' and

‘***’ indicate P<0.05 and 0.001, respectively. Numbers on the top of the bars indicate P values, and n.s. represents not significantly different.

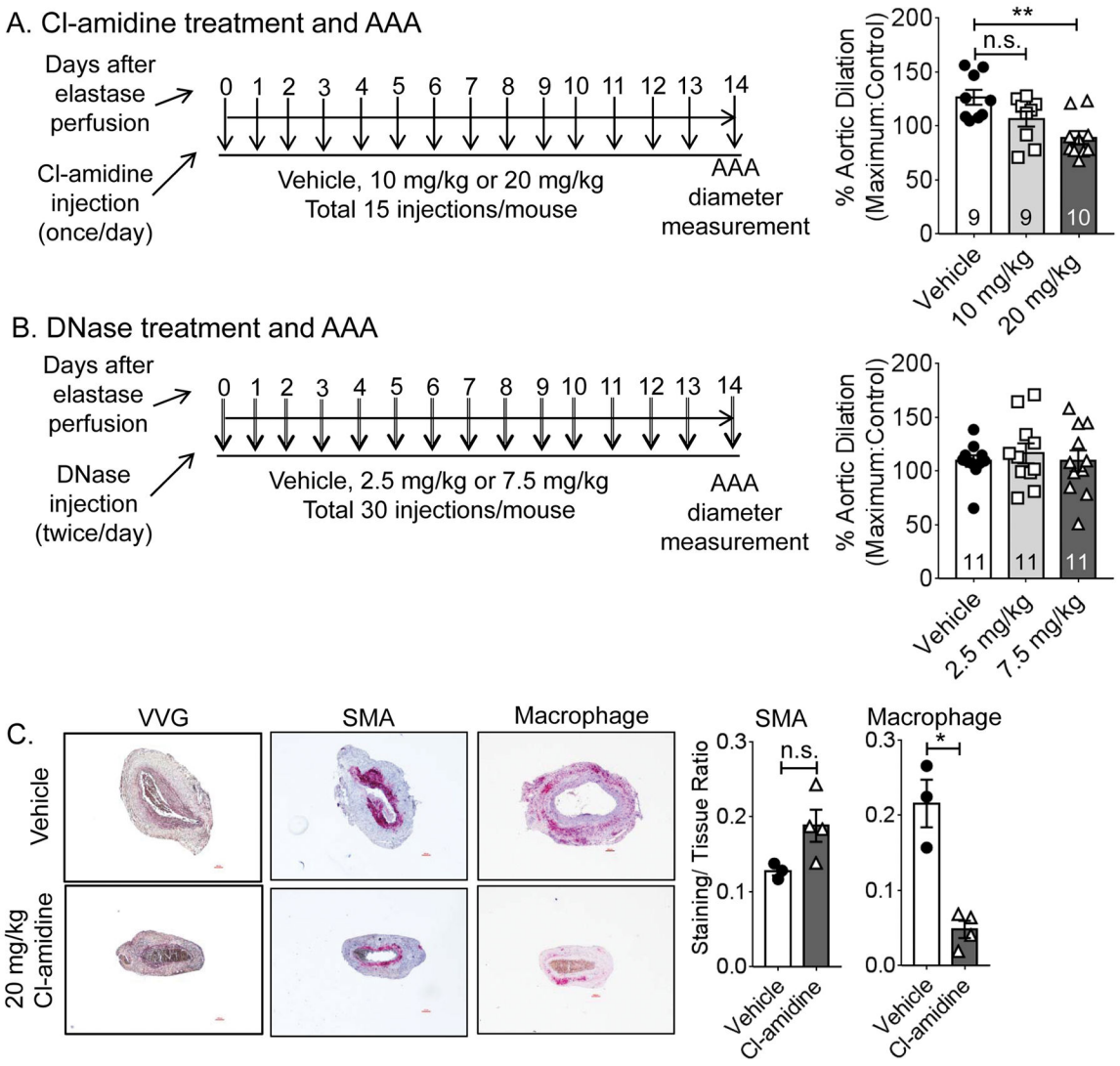

Figure 5. Cl-amidine, but not DNase injection attenuates AAA formation in WT mice

(**A**), AAA was induced in WT mice and aortic dilation was determined after 14 days. The mice received daily injection of saline (Vehicle) or two different doses of Cl-amidine from day 0 to day 14. (**B**), AAA was induced in WT mice and aortic dilation was determined after 14 days. The mice received two injections/day of saline (Vehicle) or two different doses of DNase from day 0 to day 14. (**C**), AAA pathology from the vehicle or neutrophil adoptive transferred mice was determined by Verhoeff-Van Gieson (VVG), smooth muscle α-actin (SMA, red) and macrophage (F 4/80, red) staining. Right panels, quantification of SMA and macrophage staining area, n=3–4/group. Values are expressed as means±SE and n=10–11. Scale bar, 100 μm. In **A** and **B**, the number of mice used in each group is indicated within the bars. Significant difference between the two groups was determined by a normality test (D'Agostino & Pearson, alpha=0.05, for **A** and **B**; Shapiro-Wilk, alpha=0.05, for **C**) followed by unpaired t-test with Welch's correction (F test to compare variances was not

significantly different). '*' and '**' indicate P<0.05 and 0.01, respectively. Numbers on the top of the bars indicate P values.